7-2016

Ultrahigh Sensitivity of Anomalous Hall Effect Sensor Based on Cr-Doped Bi2Te3 Topological Insulator Thin Films

Y. Ni
Iowa State University

Zhao Zhang
Iowa State University, zzhang@iastate.edu

Cajetan I. Nlebedim
Ames Laboratory, nlebedim@iastate.edu

David C. Jiles
Iowa State University, dcjiles@iastate.edu

Ultrahigh Sensitivity of Anomalous Hall Effect Sensor Based on Cr-Doped Bi2Te3 Topological Insulator Thin Films

Abstract
Anomalous Hall effect (AHE) was recently discovered in magnetic element-doped topological insulators (TIs), which promises low power consumption and high efficiency spintronics and electronics. This discovery broadens the family of Hall sensors. In this paper, AHE sensors based on Cr-doped Bi2Te3 topological insulator thin films are studied with two thicknesses (15 and 65 nm). It is found, in both cases, that ultrahigh Hall sensitivity can be obtained in Cr-doped Bi2Te3. Hall sensitivity reaches 1666 Ω/T in the sensor with the 15 nm TI thin film, which is higher than that of the conventional semiconductor HE sensor. The AHE of 65 nm sensors is even stronger, which causes the sensitivity increasing to 2620 Ω/T. Furthermore, after comparing Cr-doped Bi2Te3 with the previously studied Mn-doped Bi2Te3 TI Hall sensor, the sensitivity of the present AHE sensor shows about 60 times higher in 65 nm sensors. The implementation of AHE sensors based on a magnetic-doped TI thin film indicates that the TIs are good candidates for ultrasensitive AHE sensors.

Keywords
Anomalous Hall effect sensor, topological insulators, thin films, sensitivity

Comments
This is a manuscript of an article published as Ni, Y., Z. Zhang, I. C. Nlebedim, and D. C. Jiles. "Ultrahigh Sensitivity of Anomalous Hall Effect Sensor Based on Cr-Doped Bi 2 Te 3 Topological Insulator Thin Films." IEEE Transactions on Magnetics 52, no. 7 (2016): 1-4. DOI: 10.1109/TMAG.2016.2519512. Posted with permission.

Ultrahigh Sensitivity of Anomalous Hall Effect Sensor Based on Cr-doped Bi_2Te_3 Topological Insulator Thin Films

Y. Ni[1], Z. Zhang[1], I. C. Nlebedim[2, 1] and D. C. Jiles[1], *Fellow, IEEE*

[1] Department of Electrical and Computer Engineering, Iowa State University, Ames, IA 50011 USA
[2] Ames Laboratory, U.S. Department of Energy

Anomalous Hall effect (AHE) is recently discovered in magnetic element doped topological insulators (TIs), which promises low power consumption and high efficiency spintronics and electronics. This discovery broadens the family of Hall sensors. In this work, AHE sensors based on Cr doped Bi_2Te_3 topological insulator thin films are studied with two thicknesses (15 nm and 65 nm). It is found in both cases that ultrahigh Hall sensitivity can be obtained in Cr doped Bi_2Te_3. Hall sensitivity reaches 1666 Ω/T in sensor with 15nm TI thin film which is higher than that of the conventional semiconductor Hall effect sensor. The anomalous Hall effect of 65 nm sensors is even stronger, which causes the sensitivity increasing to 2620 Ω/T. Moreover, after comparing Cr doped Bi_2Te_3 with previously studied Mn doped Bi_2Te_3 TI Hall sensor, the sensitivity of present AHE sensor shows about 60 times higher in 65 nm sensors. The implementation of AHE sensors based on magnetic doped TI thin film indicates that the TIs are good candidates for ultra-sensitive AHE sensors.

***Index Terms*— Anomalous Hall effect sensor, topological insulators, thin films, sensitivity.**

Corresponding author: Z. Zhang (e-mail: zhenn.zhang@gmail.com).

I. Introduction

Since the discovery of the Hall effect (HE), its scientific meaning as well as practical application has always been an interesting topic to researchers. Most commercial used Hall sensor nowadays are semiconductor material based on it low carrier density and high carrier mobility such as GaAs [1]. However, the high resistance and low response frequency of semiconductor limit its application in industry [2]. Besides using Lorenz force causing charge accumulation to achieve Hall in semiconductor, there is a emergent developing field known as spin-dependent HE including quantum Hall effect (QHE), anomalous Hall effect (AHE) and spin Hall effect (SHE) [3]. Ultrahigh AHE sensitivity has been reported in various metallic heterostructure and metal-oxide interfaces [4-6]. Already achieved sensitivity of the AHE-based devices exceeds 1000 Ω/T, which surpasses the sensitivity of semiconducting Hall sensors [4]. It is believed that the AHE is an alternative approach to largely increase the Hall sensitivity and response frequency while keeping the low power consumption.

Recently, quantum AHE has been experiment observed in Topological insulator which broadens the horizon of the AHE sensor. TI is a kind of quantum material which possesses an ultra-high carrier mobility at surface while insulating in the bulk because of spin-polarized massless Dirac surface state [7]. Moreover, after introducing magnetic element into TI, quantum anomalous Hall effect (QAHE) appears in ferromagnetic TI system because the suppression of one spin channel[8-10]. The discovery of TIs broadens spin-dependent electronics and devices[11, 12]. Bi_2Te_3, Bi_2Se_3, Sb_2Te_3 were reported as 3D TI which confirmed by ARPES and magneto-transport measurements [13, 14]. It has been reported that in Mn doped TI, the Hall sensitivity increase 8 times caused by QAHE [15]. However, the sensitivity of Mn doped TI AHE sensor is much lower than other AHE sensor reported. Previously work on Cr doped Bi_2Te_3 [16] shows that Cr introduces much stronger magnetization in the system than Mn indicating that the sensitivity of AHE sensor based on it will be very high. In order to seek a much higher sensitivity AHE senor based on TI, in this work, we fabricate Hall effect sensors based on Cr-doped Bi_2Te_3 TI thin films. The sensitivity, Hall resistivity, coercivity, electrical property, and temperature dependence of sensors will be studied.

II. Experiment

$Cr_xBi_{2-x}Te_3$ thin films were deposited on preheated mica substrate by Perkin-Elmer 430 molecular beam epitaxy. Mica substrate was cleaved freshly and load into the growth chamber before depositions. Mica substrate was heated to 235ºC and wait until stable. Two sets of samples with the same atom fraction (x) of 0.14 have been grown with 30min and 2hour growth time. High purity source materials (Cr, Bi and Te) was placed in the effusion Cells and heated during the growth. The flux ratio of Te per Bi was set to approximately 10 in the growth chamber to maintained Te-rich environment in order to reduce the Te vacancies. Cr concentration was controlled by adjusting the cell temperature. The thickness of the thin film was controlled by deposition duration and monitored by reflection high energy electron diffraction (RHEED).

Crystalline structure of the as-grow thin films were characterized by X-ray Diffractometer (Siemens D500 XRD) at room temperature. Atomic force microscopy (AFM) was used to demonstrate the surface morphology and roughness of sensors. The concentration of Cr concentration was determined by FEI Quanta FE-EDX. Hall effect sensor was then fabricated based on the thin film as follows. First, the Hall bar geometry was defined by reactive-ion etching (RIE) method with Ar gas. Then, the magneto transport was performed on the as-made Hall effect sensor. Hall resistance (R_{xy}) and longitudinal magnetoresistance (R_{xx}) were measured by a Quantum Design Physical Property Measurement System (PPMS) with the excitation current flowing in the film plane and the magnetic field applied perpendicular to the plane shown inset of Fig. 4.

III. Results and Discussion

A. Surface morphology and crystal structure of $Cr_{0.14}Bi_{1.86}Te_3$ Hall effect sensors

Figure 1(a) and 1(b) shows the surface morphology of $Cr_xBi_{2-x}Te_3$ topological insulator thin film for the sensor with different growth duration. The AFM image shows triangle terrace-like surface for both samples indicating a layer-by-layer epitaxy mechanism. However, different terrace width can be detected between two samples. The terrace width of sensor with 2hour growth time is about 300nm which is about 10 times larger than 30min growth time. The thickness of the two samples can also be obtained by scratching the surface and scanning by AFM. The results are shown in Figs. 1(c) and (d). The dark regions indicate the film been removed and the step in the curve shows the thickness is approximate 15 nm and 65 nm for a 30min and 2 hour sample respectively. The growth rate then can be calculated to be 0.52nm/min. The RMS roughness for both samples is under 1nm indicating the good quality of sample for device applications.

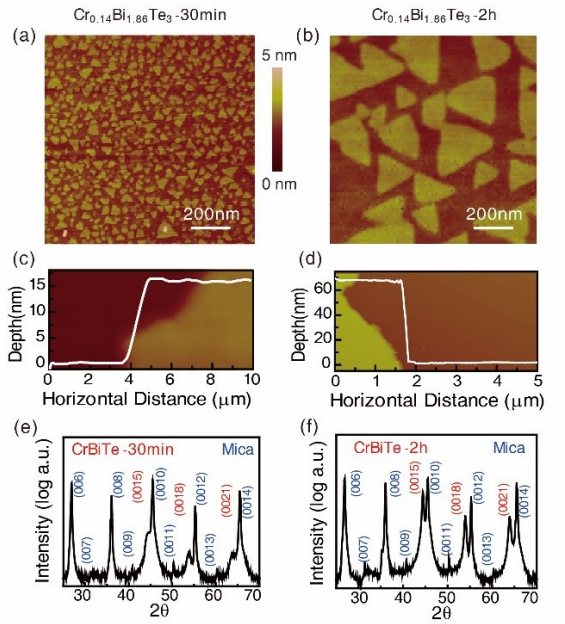

Fig. 1. Characterization of $Cr_{0.14}Bi_{1.86}Te_3$ based sensors with different deposition duration. (a) and (b) surface morphology; (c) and (d) thickness; (e) and (f) X-ray diffraction patterns of sensors with 30min and 2hour growth, respectively.

The crystal structure analysis is shown in Figs. 1(e) and (f). Two sets of diffraction peaks are observed for both samples. One set of these diffraction peaks can be indexed as mica substrate; while (0015), (0018) and (0021) diffraction peaks are obtained from $Cr_{0.14}Bi_{1.86}Te_3$ thin films with rhombohedral structure. Since the low thickness of thin films, the X-ray penetrates the thin film and detected both mica substrate and sample. It is noticed that the intensity of thicker sample is higher than that of the thinner sample. No extra peak is observed in both samples indicating the thin film is highly orientated. From the strongest peaks (0015), (0018) and (0021) of $Cr_{0.14}Bi_{1.86}Te_3$, the *c*-axis lattice constant can be calculated as 30.5 Å, which is larger than that of the pure Bi_2Te_3 (*c* = 28.8 Å). This lattice expansion of Cr doped Bi_2Te_3 indicates that Cr not only substitutes into the Bi site but also trapped in the Van de Waals gap between layers. To summary, all the characterization results demonstrate that the $Cr_{0.14}Bi_{1.86}Te_3$ thin film with thickness of 15nm and 65nm are in high quality and suitable candidate for HE sensors.

B. Magneto-transport properties of $Cr_{0.14}Bi_{1.86}Te_3$ Hall effect sensors

After characterizing thin films, HE sensors are fabricated and magneto-transport measurements are carried out. Figure 2 shows Hall resistivity results at different temperatures from 20K to 2.5K. At 20K, the Hall resistivity (ρ_{xy}) varies between sensors with different thicknesses. The 15nm thin film sensor shows linear behavior of ρ_{xy} and almost field independence. Whereas the 65nm thin film sensor shows nonlinear behavior in ρ_{xy} and a positive slope of ρ_{xy} regarding to magnetic field, indicating the sample has similar HE as a p-type semiconductor and it is difficult to observe QAHE in present samples. The appearance of nonlinearity in at large magnetic field indicates Cr appears to substitute in Bi site and a net magnetization is generated in the thick sample at this temperature.

With decreasing the testing temperature to 10K, both 15nm and 65nm sample show hysteresis behavior with small coercivity which indicates that AHE happens at this temperature due to a paramagnetic to ferromagnetic phase transition [17]. As can be observed that ρ_{xy} saturated at a certain magnetic field. The saturation Hall resistivity (ρ_{xy}^{s}) of 65nm sample is much larger than that of 15nm sample. The Hall resistivity shows more obvious hysteresis behavior when temperature drops further down to 7.5K and 2.5K.

At lowest testing temperature in present work (T = 2.5K), the hysteresis behavior with relative large coecivity can be observed both in thick and thin sensors. For AHE, Hall resistance is described as $\rho_{xy}=R_H H+R_{AH}(M)$, which is composed of both ordinary Hall resistivity $R_H H$ and anomalous Hall resistivity $R_{AH}(M)$. Here, $R_{AH}(M)$ takes the dominant role in Hall resistivity. Since the magnetization of sensors behaves hysterically, the ρ_{xy} also shows the hysteresis behavior. Obviously, in all testing temperature range in this work, the saturation Hall resistivity (ρ_{xy}^{s}) of 65nm sensor is much larger than that of the 15nm sample. This may result from the magnetic anisotropy of the thin sample is different from that of the thick samples [18].This different can be further explained by comparing ρ_{xy}^{s} of these two sensors at different temperature.

Figure 2(f) shows the temperature dependence of saturation Hall resistivity (ρ_{xy}^{s}). Both sensors with thinner and thicker film show a rapid decrease when near 8K indicating the ferromagnetic phase transition happened around this temperature (Tc), which generate magnetization after the phase transition contribute to AHE effect in $Cr_{0.14}Bi_{1.86}Te_3$ sensors [17]. The highest saturation Hall resistivity in 15nm sensor is about 27 μΩ•cm at 2.5K which is larger than that of Mn doped Bi_2Te_3 AHE sensor. Moreover, the largest value reaches to 225 μΩ•cm in 65nm sensor. The large difference between the 15nm sensor and 65nm sensor demonstrate that a magnetic easy axis in the plane when thickness is about 15nm whereas a perpendicular magnetic anisotropy (PMA) has been obtained when the $Cr_{0.14}Bi_{1.86}Te_3$ sensor thickness reach 65nm which is the similar to the AHE senor with CoFeB and PtFe thin film [19] And more values of thickness will be performed in our future works to reveal this interesting phenomenon in detail.

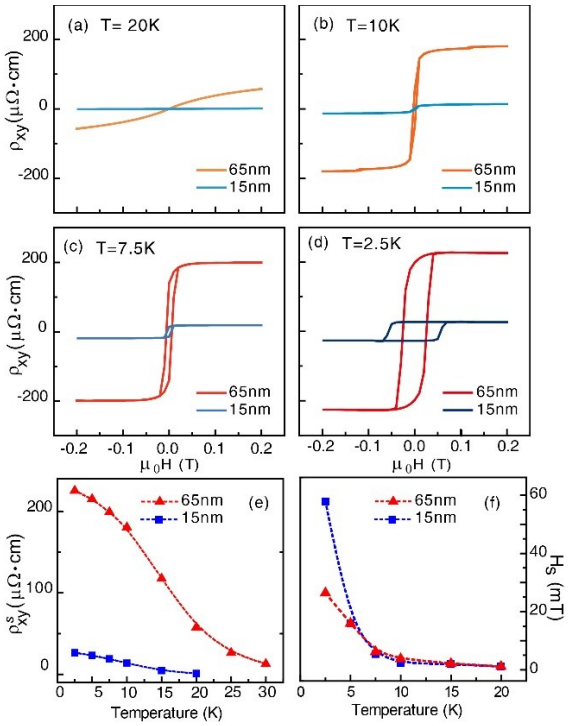

Fig. 2. Temperature dependence of Hall resistance curves for $Cr_xBi_{2-x}Te_3$ HE sensor with different thickness. (a) T = 20K, (b) T = 10K, (c) T = 7.5K, and (d) T= 2.5K. (e) Temperature dependence of saturation field for $Cr_xBi_{2-x}Te_3$ HE sensor and (f) saturation Hall resistivity at zero magnetic field. The dashed lines in (e) and (f) are guides to the eye.

Another crucial characteristic of AHE sensor is the saturation field (H_s). Fig.2 (e) is the summary of H_s as temperature varying from 2.5K to 30K. Both of the two samples show a decrease tendency of H_s when temperature increase which is similar to typical ferromagnetic materials [20]. An abrupt change of H_s can be observed at about 8K for both samples, consisting with the curie temperature (Tc) shown in ρ^s_{xy} . The lowest H_s for both thin film sensors is below 10mT, which exhibits low switching field superiority for the device application [19]. The high saturation Hall resistivity and low saturation field imply the ultrahigh sensitivity in $Cr_xBi_{2-x}Te_3$ based sensor.

The carrier density can be extracted from the Hall measurement by using: $n=(|R_H|e)^{-1}$, where R_H is the Hall coefficient and e is the electron charge. Fig.3 (a) shows temperature dependent carrier density. As temperature increases the carrier density also increasing. The thinner sample has higher carrier density of than the thicker sample because *n* is inverse proportional to ρ_{xy} . Since ρ_{xy} of thin sample is smaller than that of the thick sample, *n* is larger. The lowest carrier density can achieve 0.55×10^{18} cm^{-3}. The carrier mobility [Fig.3 (b)] of $Cr_{0.14}Bi_{1.86}Te_3$ TI sensor is calculated by using: $\mu=\frac{\sigma_{xx}}{ne}$, where σ_{xx} is the longitudinal conductivity. The mobility decrease from 0.35 m^2/Vs to 0.02 m^2/Vs with temperature increase from 2.5K to 30K for 65nm sample. For the 15nm sample, similar trend can be observed with lower value of carrier mobility, ranging from 0.16 to 0.006 m^2/Vs. The highest carrier mobility are comparable to pure Bi_2Te_3 in which the effective mass of charge carrier is almost zero[21]. The relative low carrier density and high carrier mobility are signs of high Hall sensitivity.

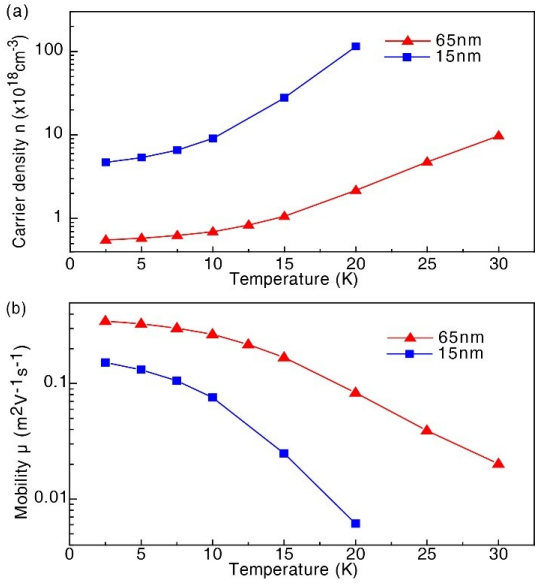

Fig. 3. Carrier density(a) and carrier mobility(b) of TI AHE sensor with 15nm and 65 nm thickness $Cr_xBi_{2-x}Te_3$ thin film.

C. *The effect of temperature on sensitivity of $Cr_xBi_{2-x}Te_3$ Hall effect sensors*

The most important characteristic parameters of HE sensor is Hall sensitivity (S), which is the figure of merit for Hall sensor. The sensitivity of AHE sensors can be defined as initial Hall slope $S=d\rho_{xy}/dH$. Based on the magneto-transport properties shown in Fig. 2, Hall sensitivity of $Cr_{0.14}Bi_{1.86}Te_3$ sensors with different thickness can be calculated.

Figure 4 shows sensitivity of sensors within saturation field as a function of temperature and thickness. Inset of Fig. 4 shows the schematic picture of Hall sensor under testing. It can be observed that with temperature decreasing the sensitivity tends to increase. Below the temperature (T = 8K), sensitivity suddenly jumped to magnitude higher than that of the higher temperatures. This is because doping Cr introduces magnetization after ferromagnetic phase transition causing AHE. The thinner TI sensor (15nm) shows the highest sensitivity S = 1666 Ω/T at T = 2.5K, surpassing the highest sensitivity of semiconductor HE sensor (1000 Ω/T) [22]. At T = 2.5K, the sensitivity reaches 2620 Ω/T in 65nm sensor which is twice higher than 15nm sample. Moreover, Fig. 4 also compares the sensitivity between Cr doped Bi_2Te_3 and Mn doped Bi_2Te_3, of which the sensitivity is in the range 5 Ω/T - 43 Ω/T [15]. The sensitivity of 65nm $Cr_{0.14}Bi_{1.86}Te_3$ AHE sensor is about 60 times higher than that of Mn doped Bi_2Te_3 AHE sensor, which may due to the more stable ferromagnetism and insulation of $Cr_{0.14}Bi_{1.86}Te_3$. It should be mentioned that in the temperature range from 2.5K to 10K, sensitivity keep higher than 2000 Ω/T. This low temperature

AHE sensor can be used as cryogenic magnetic field measurements, research of superconducting materials and low temperature magnetometry measurements.

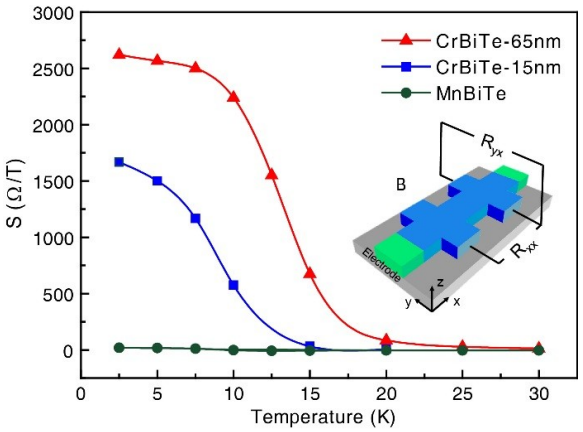

Fig. 4. Temperature dependence of sensitivity for $Cr_xBi_{2-x}Te_3$ AHE sensor with different thickness. Inset shows the schematic picture of HE sensor under testing. The green curve shows the Mn doped Bi_2Te_3 topological insulator thin film with similar testing condition.

IV. Conclusion

To summarize, we studied AHE sensor based on $Cr_xBi_{2-x}Te_3$ topological insulator with thickness of 15 nm and 65 nm. It is found that the sensor remains high sensitivity in both thicknesses. The giant sensitivity is found S=2620 Ω/T at 2.5K in $Cr_xBi_{2-x}Te_3$ sensor with thickness of 65 nm which is more than twice the sensitivity of semiconductor HE sensor. The high sensitivity results from Cr induced AHE in TI thin films. The $Cr_xBi_{2-x}Te_3$ sensors show high carrier mobility, which enables the application of low power consumption magnetic sensors. Moreover, both saturation Hall resistivity and sensitivity show dependence on thickness, which indicates the variation of magnetic anisotropy with changing thickness in sensors. Our work therefore enlightens the design of low-energy consumption and high sensitivity Hall devices such as magnetic sensor and memory devices.

Acknowledgment

This work was supported in part by the Division of Electrical, Communications and Cyber Systems, U.S. National Science Foundation under Grant 1201883. Magnetotransport analysis performed at Ames was supported by the U.S. DOE, Office of Science, Basic Energy Sciences, Materials Science and Engineering Division. Ames Laboratory is operated for the U.S. DOE by Iowa State University under contract DE-AC02-07CH11358.

References

[1] R. S. Popovic, *Hall effect devices*: CRC Press, 2003.

[2] E. Ramsden, *Hall-effect sensors: theory and application*: Newnes, 2011.

[3] Y. Kato, R. Myers, A. Gossard, and D. Awschalom, "Observation of the spin Hall effect in semiconductors," *Science*, vol. 306, pp. 1910-1913, 2004.

[4] Y. Lu, J. Cai, H. Pan, and L. Sun, "Ultrasensitive anomalous Hall effect in SiO2/Fe-Pt/SiO2 sandwich structure films," *Appl. Phys. Lett.* vol. 100, p. 022404, 2012.

[5] S. Zhang, J. Teng, J. Zhang, Y. Liu, J. Li, G. Yu, and S. Wang, "Large enhancement of the anomalous Hall effect in Co/Pt multilayers sandwiched by MgO layers," *Appl. Phys. Lett.*, vol. 97, p. 222504, 2010.

[6] S. Ikeda, K. Miura, H. Yamamoto, K. Mizunuma, H. Gan, M. Endo, S. Kanai, J. Hayakawa, F. Matsukura, and H. Ohno, "A perpendicular-anisotropy CoFeB–MgO magnetic tunnel junction," *Nat. Mater.*, vol. 9, pp. 721-724, 2010.

[7] M. Z. Hasan and C. L. Kane, "Colloquium: topological insulators," *Rev. Mod.Phys.*, vol. 82, p. 3045, 2010.

[8] C.-Z. Chang, J. Zhang, X. Feng, J. Shen, Z. Zhang, M. Guo, K. Li, Y. Ou, P. Wei, and L.-L. Wang, "Experimental observation of the quantum anomalous Hall effect in a magnetic topological insulator," *Science*, vol. 340, pp. 167-170, 2013.

[9] S.-G. Cheng, "The quantum anomalous Hall effect in a topological insulator thin film—The role of magnetic disorder," *EPL*, vol. 105, p. 57004, 2014.

[10] M. Onoda and N. Nagaosa, "Topological nature of anomalous Hall effect in ferromagnets," *J. Phys. Soc. Japan*, vol. 71, pp. 19-22, 2002.

[11] T. Fujita, M. B. A. Jalil, and S. G. Tan, "Topological insulator cell for memory and magnetic sensor applications," *Appl. Phys. Express*, vol. 4, p. 094201, 2011.

[12] M. B. Jalil, S. Tan, and Z. Siu, "Quantum anomalous Hall effect in topological insulator memory," *J.Appl. Phys.*, vol. 117, p. 17C739, 2015.

[13] D.-X. Qu, Y. Hor, J. Xiong, R. Cava, and N. Ong, "Quantum oscillations and Hall anomaly of surface states in the topological insulator Bi_2Te_3," *Science*, vol. 329, pp. 821-824, 2010.

[14] J. Zhang, C.-Z. Chang, Z. Zhang, J. Wen, X. Feng, K. Li, M. Liu, K. He, L. Wang, and X. Chen, "Band structure engineering in $(Bi_{1-x}Sb_x)_2Te_3$ ternary topological insulators," *Nat. Commun.*, vol. 2, p. 574, 2011.

[15] Y. Ni, Z. Zhang, I. C. Nlebedim, R. L. Hadimani, and D. C. Jiles, "Influence of Mn Concentration on Magnetic Topological Insulator $Mn_xBi_{2-x}Te_3$ Thin-Film Hall-Effect Sensor," *IEEE Trans. Magn.*, vol. 51, pp. 1-4, 2015.

[16] Y. Ni, Z. Zhang, I. Nlebedim, R. Hadimani, G. Tuttle, and D. Jiles, "Ferromagnetism of magnetically doped topological insulators in $Cr_xBi_{2-x}Te_3$ thin films," *J. Appl. Phys.* vol. 117, p. 17C748, 2015.

[17] R. Yu, W. Zhang, H.-J. Zhang, S.-C. Zhang, X. Dai, and Z. Fang, "Quantized Anomalous Hall Effect in Magnetic Topological Insulators," *Science*, vol. 329, pp. 61-64, 2010.

[18] S. Ikeda, K. Miura, H. Yamamoto, K. Mizunuma, H. D. Gan, M. Endo, S. Kanai, J. Hayakawa, F. Matsukura, and H. Ohno, "A perpendicular-anisotropy CoFeB–MgO magnetic tunnel junction," *Nat. Mater.*, vol. 9, pp. 721-724, 2010.

[19] T. Zhu, P. Chen, Q. Zhang, R. Yu, and B. Liu, "Giant linear anomalous Hall effect in the perpendicular CoFeB thin films," *Appl. Phys. Lett.*, vol. 104, p. 202404, 2014.

[20] Y. Ni, Z. Zhang, C. I. Nlebedim, and D. C. Jiles, "Influence of Ga-concentration on the electrical and magnetic properties of magnetoelectric $CoGaxFe_{2-x}O_4/BaTiO_3$ composite," *J. Appl. Phys.*, vol. 117, p. 17B906, 2015.

[21] K. Wang, Y. Liu, W. Wang, N. Meyer, L. Bao, L. He, M. Lang, Z. Chen, X. Che, and K. Post, "High-quality Bi_2Te_3 thin films grown on mica substrates for potential optoelectronic applications," *Appl. Phys. Lett.* vol. 103, p. 031605, 2013.

[22] J.-S. Lee, K.-H. Ahn, Y.-H. Jeong, and D. M. Kim, "Quantum-well Hall devices in Si-delta-doped $Al_{0.25}Ga_{0.75}As$/GaAs and pseudomorphic $Al_{0.25}Ga_{0.75}As/In_{0.25}Ga_{0.75}As$/GaAs heterostructures grown by LP-MOCVD: performance comparisons," *IEEE Trans. Electron Dev.*, vol. 43, pp. 1665-1670, 1996.